ARTICLE

Investigation on Excited-State Photophysical Characteristics of Low Bandgap Polymer APFO3

Li-li Qu[a], Ying-hui Wang[a,b*], Zhi-hui Kang[a], Yu-guang Ma[b], Han-zhuang Zhang[a*]

a. Femtosecond laser laboratory, College of Physics, Jilin University, Changchun 130012, China
b. State Key Laboratory of Supramolecular Structure and Materials, Jilin University, Changchun 130012, China

(Dated: Received on June 25, 2013; Accepted on August 7, 2013)

The excited state photophysics of low bandgap polymer APFO3 has been investigated in detail. The chemical calculations confirm that the intrachain charge transfer (ICT) may occur after photo-excitation and is mainly responsible for the first absorption band. The transient absorption results confirm that ICT indeed exists and competes with the vibrational relaxation at the same time, when APFO3 is in a monodisperse system. This ICT process would disappear due to the influence of interchain interaction when APFO3 is in the condensed phase, where the exciton decay would be dominant in the relaxation process after photoexcitation. The photoexcitation dynamics of APFO3 film blending with $PC_{61}BM$ are presented, which shows that the exciton may be dissociated completely as the percentage of $PC_{61}BM$ reaches ∼50%. Meanwhile, the photovoltaic performance based on blend heterojunction shows that the increase of photocurrent is little if the percentage of $PC_{61}BM$ exceeds ∼50%. Overall, the present study has covered several fundamental processes taking place in the APFO3 polymer.

Key words: Conjugated polymer, Transient absorption, Intrachain charge transfer

I. INTRODUCTION

Semiconductor polymers have attracted much attention in the fields of commerce and science, because of their potential application in the optoelectronic fields, such as organic field effect transistor [1], organic emitting light diode [2], and polymer solar cell [3]. These organic materials own many advantages over conversional semiconductors, such as the good solution processability and the mechanical properties, and are able to allow access to generation of cheap and flexible devices. Recently, the solar cells based on polymer have increased very much and reached ∼10% in 2012 [4]. In order to further improve the performance of photovoltaic devices, it is necessary to synthesize the low-bandgap polymers, so as to broaden the harvesting region of photon and enhance the short circuit current of photovoltaic device [5]. The alternating polyfluorene copolymer (poly[(9,9-dioctylfluorenyl-2,7-diyl)-alt-5,5-(4′,7′-di-2-thienyl-2′, benzothiadiazole)]) (APFO3), with structure shown in Fig.1, is one kind of π-conjugated copolymers, which is composed of the electron-donor unit (fluorine group) and the electron-acceptor units (benzothiadiazole and two thiophene units). Its absorption bandedge has reached ∼700 nm in the solution and its carrier mobility is also excellent, which makes it suitable for photovoltaic application [7]. In addition, APFO3 has also been used as a model polymer to investigate the charge transfer and geminate recombination processes occurring in the polymer blending heterojunction with $PCB_{60}M$ [8] and $PCB_{70}M$ [9]. Although the photophysics of heterojunction based on APFO3 have been investigated in detail, some questions still need to be interpreted, such as evolution of photophysical properties under different situations, the direct photo-generation of separated charges in the excited state, and the role and origin of possible interchain electronic species. In order to answer these questions, it is necessary to present a broad investigation on this conjugated polymer and compare the photoexcitation dynamics of conjugated polymer under different conditions.

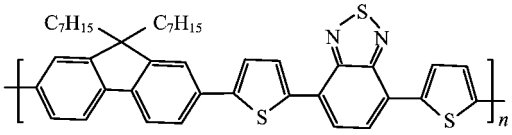

FIG. 1 Molecular structure of APFO3.

In this work, we performed a series of investigations on the photophysics of conjugated polymer APFO3 to understand its photoexcitation dynamics in a monodisperse system and a condensed phase. Through intro-

*Authors to whom correspondence should be addressed. E-mail: yinghui_wang@jlu.edu.cn, zhanghz@jlu.edu.cn

ducing the $PC_{61}BM$ in the APFO3 film, we also detected the exciton dissociation dynamics and further prepared the photovoltaic devices. In addition, we could employ the density functional theory (DFT) to know the basic electronic transition mechanism after the photoexcitation. Finally, we provided the spectroscopic studies of APFO3 in detail.

II. EXPERIMENTS

A. Materials

The chemicals used were all purchased from Lumtec Technology without further purification. The polymer dissolved in the chlorobenzene (CB) solvent with concentration of 100 μg/mL. The APFO3 and APFO3:$PC_{61}BM$ thin films were prepared through spin coating the sample solution in the CB solution onto 2 mm thick fused silica glass substrates.

B. Experimental details

Steady-state absorption measurements were carried out using a UV-Vis spectrophotometer (Purkinje, TU-1810PC). Photoluminescence (PL) spectra were recorded by a fiber optic spectrometer (Ocean Optics, USB4000) with excitation pulse at 400 nm. We employed a mode-lock Ti:Sapphire femtosecond laser system (Coherent), which offered 2.0 mJ, 130 fs pulses at 800 nm with a repetition rate of 1 kHz. The setup of transient absorption (TA) measurement was reported in Ref.[10]. Briefly, the output of femtosecond laser beam was split into two parts. The major one was frequency-doubled by a 1 mm thick BBO crystal to generate 400 nm pulses, which will be used as the pump beam, while the minor one was focused into a 5 mm quartz cell filled with pure water to generate a white light continuum as the probe beam. The probe beam was also focused onto the sample to overlap with the pump beam. The transmittance change of probe pulse was detected by a photomultiplier tube (Zolix, PMTH-S1-CR131) connected to the lock-in Amplifier (SR830, DSP). Photovoltaic devices were comprised of thin film with indium tin oxide (ITO) anode, PEDOT:PSS hole transport layer, active layer of spin-coated PDPP-F/$PC_{61}BM$ blend, and capped with Al cathode. The *J-V* (current density-voltage) characteristics of photovoltaic device were tested under sun-like illumination. The light source was a Xenon lamp with an AM1.5G filter of which intensity was calibrated to 100 mW/cm^2. All measurements were carried out at room temperature.

C. Computational methods

The ground geometry of $APFO3_n$ (n=1−4 repeat unit) was optimized with DFT [11], B3LYP functional [12], and 6-31G(d) basis set. All calculations were performed by the Gaussian 09 program package [13]. The influence of peripheral carbon chains was believed to be so small that such chains were replaced by H to avoid excessive computation demand. Electronic transition in the optical absorption of the $APFO3_2$ oligomer with two repeat units was computed with time-dependent DFT (TD-DFT) [14], CAM-B3LYP functional [15], and 6-31G(d) basis. The corresponding electronic properties and geometries were calculated by assuming APFO3 oligomers to be isolated molecules in the vacuum.

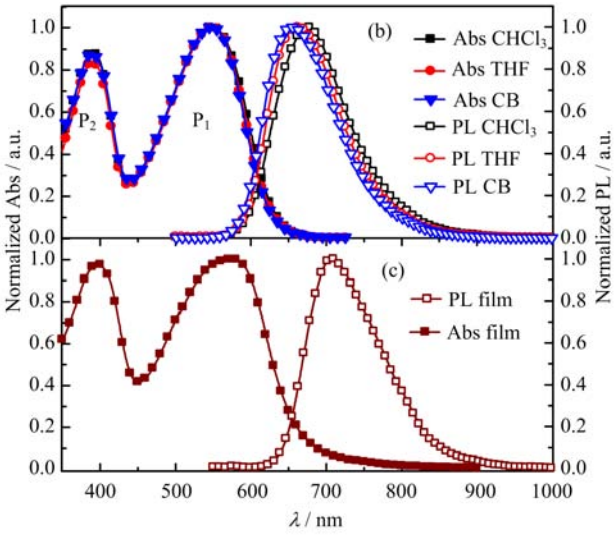

FIG. 2 Normalized absorption and emission spectra of (a) APFO3 in solution with different polarity and (b) APFO3 film (λ_{exe}=400 nm). The concentration of solution is 100 μg/mL.

III. RESULTS AND DISCUSSION

As is depicted in Fig.2(a), the absorption spectra of APFO3 in the solution with different polarity are all composed of two broad absorption bands, peaking at 389 (P_2 peak) and 548 nm (P_1 peak), respectively, which exhibits that the absorption features of APFO3 are almost independent of the polarity of solvent. Their emission spectra have a broad unstructured emission band centered at 653 nm (CB), 664 nm (THF), and 674 nm ($CHCl_3$), and their corresponding bandwidth seems to be a little narrower in comparison with that of the P_1 band in the absorption spectra. The polarity-dependent emission spectra of APFO3 show an apparent solvatochromism behavior. The emission band red shifts as the polarity of solvent gradually enhances, implying the intrachain charge transfer (ICT) may occur in this π-conjugated polymer [16]. Moreover, the emission spectra in different solvents show a good enantiomorphous feature. The bandgap could be estimated from the intersection point between the normal-

DOI:10.1063/1674-0068/27/01/109-114

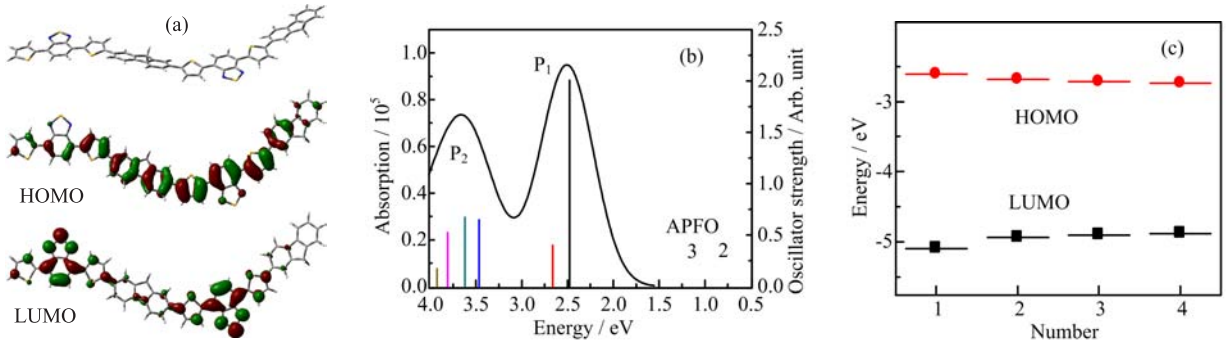

FIG. 3 (a) Optimized geometry, HOMO and LUMO of APFO3 with two repeat units. (b) Calculated absorption spectrum of APFO3 oligomer with two repeat units. (c) The repeat unit-dependent HOMO-LUMO.

ized absorption and emission spectra in Fig.2(b), which is ∼2.05 eV (CB), 2.04 eV (THF) and 2.02 eV ($CHCl_3$), respectively. The Stokes shift, given by the frequency difference between the emission maximum and the first absorption peak, is ∼2935 cm^{-1} (CB), 3188 cm^{-1} (THF) and 3412 cm^{-1} ($CHCl_3$), respectively, and gradually increases with the increasing of solvent polarity. It is noted that the geometry of D-A type conjugated polymer in excited state could be sensitive to the solvent polarity. For the APFO3 in the condensed phase, the first absorption band may broaden from ∼4083 cm^{-1} (in the solution) to ∼5234 cm^{-1}. Due to the interchain interaction, the P_1 and P_2 peaks in the absorption spectra red shift from ∼390 and ∼546.5 nm to ∼397 and ∼576 nm, respectively. Meanwhile, the emission peak also red shifts to 708 nm, the bandgap decreases to 1.89 eV, the Stokes shift changes to ∼3292 cm^{-1}.

The ground geometry of $APFO3_2$ oligomer with two repeat units is optimized by B3LYP/6-31G(d). Herein, the donor unit (fluorine group) and the acceptor units (benzothiadiazole unit and two thiophene units) all own planarity (as seen in Fig.3(a)), but a twist appears between the donor and the acceptor units. The corresponding value is ∼23.9°, which may has a little influence on the ICT character. As is seen in Fig.3(a), the highest occupied molecular orbital (HOMO) is almost distributed over the whole oligomer backbone, while the lowest unoccupied molecular orbital (LUMO) is mainly localized in the acceptor units. After photoexcitation, the charge cloud in oligomers clearly redistributes through the ICT process, and eventually the charge almost distributes on the acceptor units. The simulated absorption spectrum of $APFO3_2$ oligomer with DT-DFT/6-31G is presented in Fig.3(b), and the spectral shape with a "camel back" character is known to be a fingerprint of the donor-acceptor conjugated copolymer structure with an ICT state [17]. Similarly to the experimental data, the simulated absorption spectrum of APFO3 is also composed of two absorption band, but both of them show a little blue shift in comparison with the experimental data. According to the repeat unit-dependent HOMO and LUMO shown in Fig.3(c), we find that both of them gradually converge to an extremum and the bandgap gradually also decreases to a constant, indicating that the increase of repeat unit would lead to the red shift of the simulated absorption spectra and reduce the difference between the simulated absorption spectrum and experimental data. In addition, the calculated electronic transition is assumed to be in the vacuum, which may be also responsible for the difference between the theoretical and the experimental data. Using the calculated data for the oligomer with two repeating units, the contribution of the frontier molecular orbitals to the electronic transitions is analyzed. The low energy absorption (P_1 peak) band may be ascribed to $S_0 \rightarrow S_1$ transition and is mainly composed of HOMO→LUMO transition, where the ICT transition is dominant in $S_0 \rightarrow S_1$ transition. The high energy absorption (P_2 peak) band may be attributed to the $\pi \rightarrow \pi^*$ transition and its component is so complex, and the detailed electronic transitions in $APFO3_2$ oligomer are shown in Table I.

TABLE I Calculated transition energies E_T and oscillator strengths f for $APFO3_2$ oligomer with two repeat units.

		E_T/eV(nm)	f	Major contribution
P_1	S_1	2.4789(500.16)	2.0064	64% (H→L)
				17% (H−1→L+1)
				31% (H−1→L)
	S_2	2.6632(465.54)	0.4019	26% (H−1→L+1)
				32% (H→L+1)
P_2	S_3	3.4669(357.62)	0.6481	30% (H−2→L)
				20% (H→L+2)
	S_4	3.6225(342.26)	0.6723	21% (H−2→L+1)
				19% (H→L+2)
	S_5	3.8106(325.36)	0.5251	14% (H−3→L+1)
				19% (H→L+1)
				17% (H→L+3)
	S_6	3.9249(315.52)	0.1735	28% (H−1→L+2)
				15% (H→L+3)

The time-dependent TA spectra of the APFO3 in the

DOI:10.1063/1674-0068/27/01/109-114

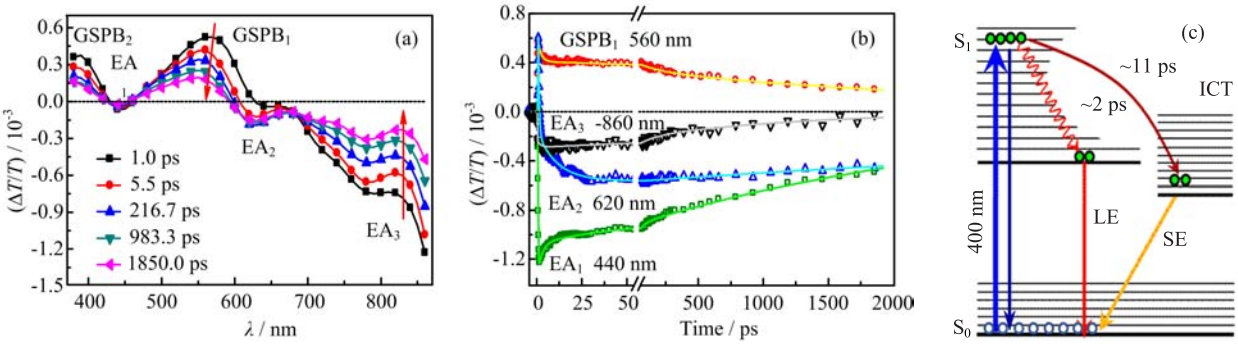

FIG. 4 (a) Time-dependent TA spectra of APFO3$_2$ in CB solution with concentration of 100 μg/mL (λ_{exe}=400 nm). (b) Temporal evolution of TA signal at λ_{probe}=440, 560, 620, and 860 nm, the solid lines are fitted results. (c) The photophysical process of APFO3$_2$ in a monodisperse system.

TABLE II Best-fit parameters of TA traces of APFO3 with multi-exponential functions.

	λ/nm	τ_1/ps	τ_2/ps	τ_3/ps	$\langle\tau\rangle$/ps
Solution	440	2.5	123	1272	
	560	1.9	145	3007	
	620	11		7613	
	860	2.0	43	2439	
Film	860	1.8(48.8%)	32(27.3%)	4038(23.9%)	974
	590	1.4(58.6%)	32(11.9%)	1639(29.4%)	486

CB solution with concentration of 100 μg/mL at different time are shown in Fig.4(a), and the aggregation between copolymer is expected to be insignificant in this concentration [18]. The TA spectrum of APFO3 at 1.0 ps has four main spectral features. Two positive absorption bands at ∼390 and ∼550 nm are attributed to ground state photo-bleaching (GSPB) because of the close resemblance to the optical absorption spectrum, and the other two negative excited absorption bands at ∼450 (EA$_1$) and above 600 nm (EA$_2$ and EA$_3$) may correspond to the excited state absorption. It is interestingly found the GSPB$_1$ gradually blue shifts from 570 nm to 550 nm with time, indicating that the simulated emission (SE) should be overlapped with the GSPB$_1$ in this spectral region. In order to understand the photophysical character of the excited APFO3, we exhibit the temporal evolution of EA$_1$, GSPB$_1$, EA$_2$, and EA$_3$ bands at selected λ_{probe}=440, 560, 620, and 860 nm, and all of them are fitted by a multi-exponential function. The fitted results are shown in Fig.4(b) and summarized in Table II. Their different decay behaviors reflect that the transient species that we are monitoring come from different energy states. The temporal trace of EA$_3$ at 860 nm shows an initial decay with the lifetime of ∼2.0 ps, showing that some transient species directly relax from the high energy excited state. Simultaneously, the dynamics of EA$_1$ also exhibit a fast rising dynamic behavior with the lifetime of ∼2.5 ps and is a little longer than that of the fast dynamic component in EA$_3$ trace, suggesting that some transient species in high energy excited state may relax to the low energy excited state through vibrational thermal relaxation. In addition, the GSPB$_1$ trace offers an initial decay with time constant ∼1.9 ps, indicating that some transient species maybe directly come back from the high energy state to the ground state. The EA$_2$ signal at 620 nm is accordingly overlapped with a residual GSPB band and displays an instantaneous formation (<0.5 ps), beyond our temporal resolution, and a slow rising component with a long lifetime of ∼11 ps, indicating that a intermediate state is generated after photoexcitation. Considering the polarity-dependent emission (Fig.2(a)) and the quantum chemical calculation (Fig.3(a)), we expect that this rising process should correspond to the inter-conversion from the initial high energy excited state to the ICT state. All the photophysical processes of APFO3 in a monodisperse system are summarized in Fig.4(c). The vibrational thermal relaxation (∼2 ps), the relaxation to the ground state, and the ICT process with lifetime of ∼11 ps may occur at the same time, and then the last transient species would all gradually come back to the ground state. Herein, our analysis provides a systemic evidence of complex relaxation processes of APFO3 polymer in the monodisperse solution system.

And then, we offer the TA spectra of the pristine APFO3 film at different times (as seen in Fig.5(a)) so as to understand the photophysical character of the excited APFO3 in the condensed phase. The TA spectrum at ∼1.0 ps has a little difference from that in the CB solution, and the component of SE disappears in the condensed phase. It contains five main spectral features: three negative bands at ∼450, 720, and 845 nm, and two positive bands at ∼410 and ∼575 nm. The positive absorption bands are also assigned to the GSPB, and three negative absorption bands are the EA part, which may correspond to the singlet-singlet ($S_1 \rightarrow S_n$) photo-induced absorption. Due to the interchain interaction, the GSPB features both red shift, meanwhile all the spectral features in TA spectra decay with time,

DOI:10.1063/1674-0068/27/01/109-114

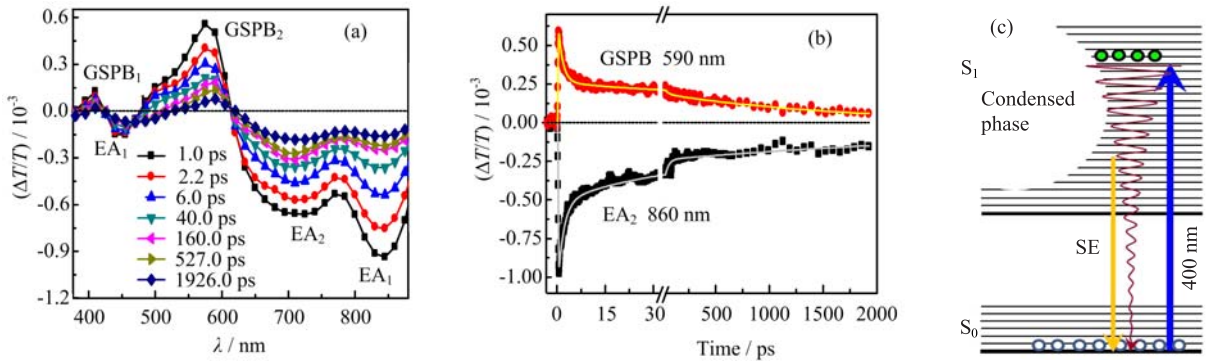

FIG. 5 (a) Transient absorption spectra of pristine APFO3 film (λ_{exe}=400 nm). (b) Wavelength-dependent TA curves of pristine APFO3 film at 590 and 860 nm. (c) The photophysical process of APFO3 in condensed system.

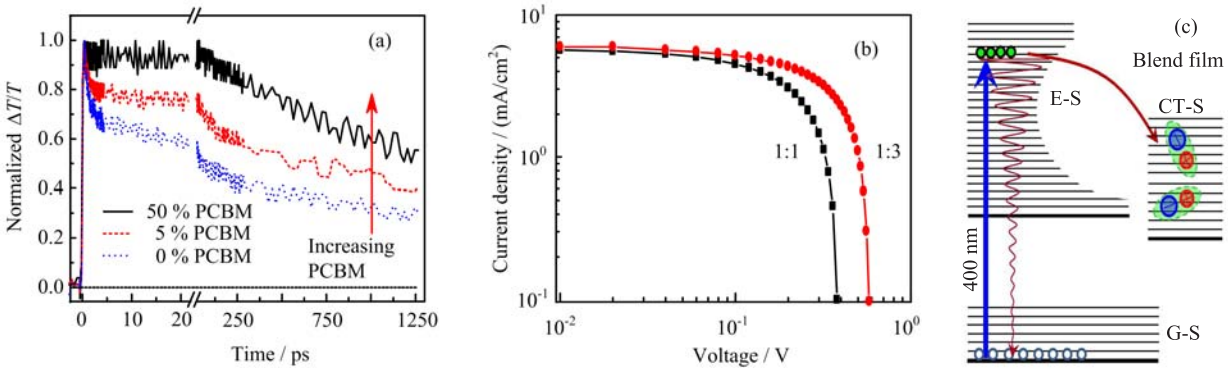

FIG. 6 (a) TA curves of pristine APFO3 and its blend films with different concentrations of $PC_{61}BM$ (λ_{exe}=400 nm). (b) Current-voltage curves measured for photovoltaic devices based on blend heterojunction (w_{APFO3}:$w_{PC_{61}BM}$=1:1 and 1:3). (c) The photophysical process of APFO3 blend film with $PC_{61}BM$.

showing that no intermediate transient species appears after photoexcitation. Note that the $GSPB_2$ and EA_3 dynamics (as depicted in Fig.5(b)), at 590 and 860 nm, respectively, display the similar temporal decay behavior, because they are both related to transitions from the first excited singlet state as depicted in Fig.5(c). At this time, the interchain exciton relaxation may be dominant in the relaxation process of excited APFO3 in the condensed phase. The dynamics of $GSPB_2$ and EA_3 are fitted by tri-exponential function and the fitted results are also summarized in Table II. There is a difference between the $GSPB_2$ dynamics ($\langle\tau\rangle\approx$486 ps) and EA_3 dynamics ($\langle\tau\rangle\approx$974 ps), which may be assigned to the superimposition of the excited state absorption and the ground state absorption. The complicated dynamic behavior of $GSPB_2$ and EA_3 indicates that there are rich dynamic processes occurring in the film at the same time, which maybe involves the excition-exction annihilation, the excition migration and the polaron relaxation.

When the APFO3 film is blended with $PC_{61}BM$, the phase segregation and the heterogeneity occur in the film morphologies. After photoexcitation, the exciton would diffuse in the polymer phase and dissociate on the interface between APFO3 and $PC_{61}BM$ phase. Figure 6(a) offer the normalized TA curves at 780 nm of the pristine APFO3 film and the blend films with different percentage of $PC_{61}BM$. After the introduction of a little $PC_{61}BM$ (5%), the component of fast exciton relaxation process obviously weakens, as presented in Fig.6(c), indicating that a part of photo-generated exciton may dissociate and form charge-transfer state (CT-S) with long lifetime. As the percentage of $PC_{61}BM$ reaches ~50%, the interface area between APFO3 and $PC_{61}BM$ increases. As seen in Fig.6(a), the fast exciton relaxation completely disappears, indicating that the photogenerated exciton has been completely dissociated after photoexcitation and the exciton dissociation yield almost reaches ~100%. In addition, the dynamic process with long lifetime should be assigned to the recombination of separated carriers. The photovoltaic devices based on blend heterojunction have been performed and the weight proportion between APFO3 and $PC_{61}BM$ is 1:1 and 1:3, so as to ensure the high effective exciton dissociation. Their current density-voltage (J-V) curves under the illumination of AM1.5G, 100 mW/cm^2 are shown in Fig.6(b). The measurement results show that V_{oc} obviously increases from 0.38 V to 0.58 V and the J_{sc} also improves from 5.84 mA/cm^2 to 5.96 mA/cm^2 as the percentage of $PC_{61}BM$ increase from 50% to 75%.

DOI:10.1063/1674-0068/27/01/109-114

Their fill factors (FF) are invariable (∼0.28). Finally, the PCE could increase from 0.61% to 1.01%. The enhancement of voltage is ∼200 mV, which may be responsible for the improvement of photovoltaic performance. The increasing of photocurrent is only 0.12 mA/cm^2 after the percentage of $PC_{61}BM$ further increases. This indicates that the increasing of $PC_{61}BM$ almost couldn't influence the generation process of free charge after the percentage of $PC_{61}BM$ has exceeded ∼50%.

IV. CONCLUSION

We systemically study the excited state photophysical character of APFO3 in the monodisperse system, the condensed phase and the mixing phase. The chemical calculations and polarity-dependent emission spectra confirm that the ICT really occurs after photoexcitation, and is mainly responsible for the first absorption band in the red region of absorption. The TA measurements confirm that ICT, as an intermediate state, really exists in a monodisperse system and competes with the vibrational thermal relaxation at the same time. Due to the influence of interchain interaction, the ICT process would disappear in the condensed phase. In addition, the photo-generated exciton could dissociate in the blended film with $PC_{61}BM$, whose yield would reach ∼100% as the percentage of $PC_{61}BM$ increases to ∼50%. The photovoltaic parameters still exhibit that the increase of photocurrent is small after the percentage of $PC_{61}BM$ exceeds ∼50%. Several fundamental situations have been covered in the study of APFO3 in excited state which is beneficial to further understand the conjugated polymers.

V. ACKNOWLEDGMENTS

This work was supported by the National Natural Science Foundation of China (No.21103161 and No.11274142) and the China Postdoctoral Science Foundation (No.2011M500927).

[1] H. Sirringhaus, P. J. Brown, R. H. Friend, M. M. Nielsen, K. Bechgaard, B. M. W. Langeveld-Voss, A. J. H. Spiering, R. A. J. Janssen, E. W. Meijer, P. Herwig, and D. M. de Leeuw, Nature **401**, 685 (1999).
[2] R. H. Friend, R. W. Gymer, A. B. Holmes, J. H. Burroughes, R. N. Marks, C. Taliani, D. D. C. Bradley, D. A. Dos Santos, J. L. Bredas, M. Logdlund, and W. R. Salaneck, Nature **397**, 121 (1999).
[3] S. E. Shaheen, C. J. Brabec, N. S. Sariciftci, F. Padinger, T. Fromherz, and J. C. Hummelen, Appl. Phys. Lett. **78**, 841 (2001).
[4] Z. C. He, C. M. Zhong, S. J. Su, M. Xu, H. B. Wu, and Y. Cao, Nat. Photon. **6**, 591 (2012).
[5] J. Peet, J. Y. Kim, N. E. Coates, W. L. Ma, D. Moses, A. J. Heeger, and G. C. Bazan, Nat. Mater. **6**, 497 (2007).
[6] C. M. Bjorstrom, A. Bernasik, J. Rysz, A. Budkowski, S. Nilsson, M. Svensson, M. R. Andersson, K. O. Magnusson, and E. Moons, J. Phys.: Conden. Mater. **17**, L529 (2005).
[7] A.Gadisa, F. L. Zhang, D. Sharma, M. Svensson, M. R. Andersson, and O. Inganas, Thin Solid Films **515**, 3126 (2007).
[8] S. De, T. Pascher, M. Maiti, K. G. Jespersen, T. Kesti, P. Zhang, O. Inganäs, A. Yartsev, and V. Sundström, J. Am. Chem. Soc. **129**, 8466 (2007).
[9] S. K. Pal, T. Kesti, M. Maiti, F. Zhang, O. Inganäs, S. Hellström, M. R. Andersson, F. Oswald, F. Langa, T. Österman, T. Pascher, A. Yartsev, and V. Sundrström, J. Am. Chem. Soc. **132**, 12440 (2010).
[10] Y. H. Wang, J. Q. Hou, Z. H. Kang, L. J. Gong, T. H. Huang, L. L. Qu, Y. G. Ma, R. Lu, and H. Z. Zhang, Chem. Phys. Lett. **566**, 17 (2013).
[11] P. Hohenberg and W. Kohn, Phys. Rev. **136**, B864 (1964).
[12] A. D. Becke, Phys. Rev. A **38**, 3098 (1988).
[13] M. J. Frisch, G. W. Trucks, H. B. Schlegel, G. E. Scuseria, M. A. Robb, J. R. Cheeseman, G. Scalmani, V. Barone, B. Mennucci,G. A. Petersson, H. Nakatsuji, M. Caricato, X. Li, H. P. Hratchian, A. F. Izmaylov, J. Bloino, G. Zheng, J. L. Sonnenberg, M. Hada, M. Ehara, K. Toyota, R. Fukuda, J. Hasegawa, M. Ishida, T. Nakajima, Y. Honda, O. Kitao, H. Nakai, T. Vreven, J. A. Jr. Montgomery, J. E. Peralta, F. Ogliaro, M. Bearpark, J. J. Heyd, E. Brothers, K. N. Kudin, V. N. Staroverov, R. Kobayashi, J. Normand, K. Raghavachari, A. Rendell, J. C. Burant, S. S. Iyengar, J. Tomasi, M. Cossi, N. Rega, J. M. Millam, M. Klene, J. E. Knox, J. B. Cross, V. Bakken, C. Adamo, J. Jaramillo, R. Gomperts, R. E. Stratmann, O. Yazyev, A. J. Austin, R. Cammi, C. Pomelli, J. W. Ochterski, R. L. Martin, K. Morokuma, V. G. Zakrzewski, G. A. Voth, P. Salvador, J. J. Dannenberg, S. Dapprich, A. D. Daniels, O. Farkas, J. B. Foresman, J. V. Ortiz, J. Cioslowski, and D. J. Fox, *Gaussian 09, Revision A02*, Wallingford CT: Gaussian, Inc., (2009).
[14] E. K. U. Gross and W. Kohn, Phys. Rev. Lett. **55**, 2850 (1985).
[15] T. Yanai, D. Tew, and N. Handy, Chem. Phys. Lett. **393**, 51 (2004).
[16] S. A. Jenekhe, L. Lu, and M. M. Alam, Macromolecules **34**, 7315 (2001).
[17] K. G. Jespersen, W. J. D. Beenken, Y. Zaushitsyn, A. Yartsev, M. Andersson, T. Pullerits, and V. Sundrström, J. Chem. Phys. **121**, 12613 (2004).
[18] N. Banerji, S. Cowan, M. Leclerc, E. Vauthey, and A. J. Heeger, J. Am. Chem. Soc. **132**, 17459 (2010).

DOI:10.1063/1674-0068/27/01/109-114